ACS OMEGA

Open Access

http://pubs.acs.org/journal/acsodf

Article

Numerical Simulation of CO_2 Dissolution and Mineralization Storage Considering CO_2-Water-Rock Reaction in Aquifers

Qingying Zuo, Yizhong Zhang,* Maolin Zhang, Bin Ju, Wenhui Ning, Xin Deng, Long Yang, and Chaofeng Pang

Cite This: *ACS Omega* 2024, 9, 45983−45995

Read Online

ACCESS | Metrics & More | Article Recommendations

ABSTRACT: CO_2 storage technology is crucial in addressing climate change by controlling the greenhouse effect. This technology involves the injection of captured CO_2 into deep saline aquifers, where it undergoes a series of reactions, such as structure binding, dissolution, and mineralization, enabling long-term storage. Typically, the CO_2 is maintained in a supercritical state, enhancing its storage efficiency. However, the efficiency can be influenced by the CO_2-water-rock reactions. Many minerals exist in rock, like calcite, dolomite, kaolinite, etc. This study introduces some chemical reactions that occur during the dissolution and mineralization of CO_2. The relationship between solubility and pressure was obtained through solubility fitting. We obtained the initial parameters of the CO_2-water-rock reaction experiment by fitting the data. These parameters can be applied to the mechanism model. This study employs the GEM module of CMG software, integrating physical parameters from the Ordos Basin's deep saline aquifers to develop a mechanism model. In this model, CO_2 injection started from the first year and continued for 20 years. This study simulated a total of 80 years of CO_2 storage. This study has elucidated how reservoir conditions and injection schemes affect the dissolution and mineralization of CO_2. This study creatively combines practical experiments and numerical simulations and uses numerical simulations to compensate for the manpower and material resources consumed in actual experiments. The research results indicate that permeability should not be too high, and an increase in porosity is beneficial for storage. As the injection rate increases, the amount of CO_2 storage increases. Top layer perforation yields lower efficiency compared to full, middle, or bottom layer perforation, with the latter providing the higher efficiency in CO_2 dissolution and mineralization. Bottom perforation is the most favorable perforation position for CO_2 storage.

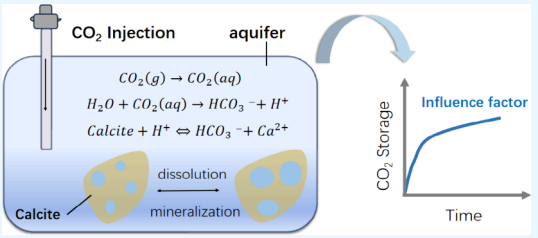

1. INTRODUCTION

Human activities have significantly increased CO_2 emissions, necessitating CO_2 storage as an effective strategy to mitigate these excessive emissions and combat global climate change.[1] Deep saline aquifers, with their vast reserves and optimal storage conditions, have emerged as the principal locations for CO_2 storage, offering a practical solution for long-term containment CO_2.[2,3] These aquifers are situated over 800 m below the surface.[4,5] They maintain a critical temperature of 31.1 °C and a critical pressure of 7.38 MPa, ensuring CO_2 remains in a supercritical state, a condition found most favorable for storage.[6,7] In this supercritical state, CO_2 exhibits unique properties: it combines the expansive compressibility typical of gases with the higher density characteristic of liquids.[8] This duality significantly enhances CO_2 diffusivity and allows for the storage of larger quantities of CO_2 within a given reservoir volume.[9−11] Thus, utilizing deep saline aquifers for CO_2 storage leverages these advantageous conditions to address the challenges posed by increased atmospheric CO_2 levels.[12,13]

The reaction between CO_2, water, and rock significantly alters the mineral composition and physical attributes of reservoir rocks, impacting the reservoir's porosity and the efficacy of CO_2 storage.[14−16] Thus, understanding the CO_2-water-rock reaction is essential when considering CO_2 storage in deep saline aquifers. Previous researchers have conducted extensive geological surveys and practical experiments for this purpose.[17,18] Duan[19] observed that formation water could dissolve significant amounts of CO_2 under high-pressure subsurface conditions, creating an acidic solution that aggressively dissolves clay minerals, such as chlorite and montmorillonite. The divalent cations required for the formation of minerals such as dolomite and siderite are released during the dissolution process (e.g., Ca^{2+}, Mg^{2+}, and Fe^{3+}). Kaszuba et al.[20] investigated geochemical reactions within sandstone-shale systems, using Acos sugar as a stand-in for natural aquifers. The experimental conditions are

Received: June 19, 2024
Revised: July 20, 2024
Accepted: November 1, 2024
Published: November 6, 2024

200 °C and 20 MPa. This research noted changes in fluid ion concentrations over time, with increases in SiO_2, K^+, and Ca^{2+} levels and decreases in Na^+ and Cl^- levels. At the end of the experiment, magnesite crystals began to form noticeably. Lahann et al.[21] studied reactions in systems combining NaCl brine, shale samples, and CO_2 at 80 °C. They observed postreaction increases in K^+, Mg^{2+}, and Ca^{2+} concentrations in the solution, unlike in control experiments without CO_2 saturation, which showed no significant changes. Luhmann et al.[22] utilized dolomite from Madison limestone for their experiments, with the experimental solution comprising 0.92 mol NaCl/kg and dissolved CO_2, maintained at 100 °C and 150 bar. They noted initial increases in cation concentrations, followed by a decrease and stabilization. Interestingly, variations in the concentrations of secondary cations like Ba^{2+}, Mn^{2+}, and Sr^{2+} were more pronounced than those of primary cations like Ca^{2+} and Mg^{2+}. The presence of localized wormholes in the rock samples indicated the occurrence of dissolution reactions.[23] The physical simulation experiment confirmed the authenticity of the CO_2-water-rock reaction. However, relying solely on actual experiments is not enough. The actual experiment requires a long time and a large amount of materials. And due to time constraints, physical experiments cannot fully simulate the entire CO_2 storage process.

Since the actual storage of CO_2 in deep saline aquifers is a process that lasts for hundreds or even thousands of years, it is necessary to conduct numerical simulation research. Numerical simulation software can simulate a long CO_2 storage process in a very short time. This greatly facilitates research on CO_2 storage. Previous researchers have conducted extensive numerical simulation work, and common software used to simulate CO_2-water-rock reactions include TOUGH, PATHARC, PRHEEQC, CMG, etc. In 1997, William D. Gunter used PATHARC software to study the reaction between industrial waste gas and typical carbonate minerals. Industrial waste gas contains CO_2, H_2SO_4, and H_2S. Carbonate minerals come from aquifers in the Alberta Basin, Canada.[24] The results showed that the reactions would generate secondary minerals such as calcite, siderite, anhydrite (gypsum), and pyrrhotite. Xu et al.[25] established a conceptual model for injecting CO_2 into sandstone shale reservoirs by utilizing common geological features and mineral compositions in sediments along the Gulf of Mexico coast. They predicted the possible dissolution and generation of minerals during the 1000-year CO_2 storage process and simulated the changes in the concentration of various ions. Cantucci et al.[26] used PRHEEQC software to simulate the Weyburn Project (Canada) case, simulating a 100-year injection of CO_2. The results showed that calcite dissolved rapidly and reached equilibrium within less than a year. Kaolinite and potassium feldspar continued to dissolve, while dolomite gradually precipitated. Turquoise mainly precipitated due to the dissolution of kaolinite, while pyrite remained unchanged. After 100 years, anhydrite or gypsum would not form. Ranganathan et al.[27] used CMG software to simulate CO_2 storage in Dutch Rottligen sandstone. Apart from quartz, the mineral composition mainly includes potassium feldspar, dolomite, kaolinite, etc. The simulation showed that the gaseous part of CO_2 migrated toward the top layer under buoyancy, while the dissolved part moved toward the middle and lower parts. The injected CO_2 was converted into kaolinite and dolomite precipitation. Numerical simulation can make it easier for people to understand the process of CO_2 storage.[28] However, these reactions simulated in numerical simulation software often lack precise parameters. Combining numerical simulation with physical simulation is a good idea. Actual experiments can obtain the exact parameters of the reaction and improve the accuracy of numerical simulations. Numerical simulation can shorten the time of actual experiments. Therefore, fitting numerical simulations with actual experiments is a feasible approach.

Beyond just numerical simulations of CO_2-water-rock reactions to evaluate mineral dissolution and precipitation, prior studies have extended to simulating and analyzing various factors that influence these reactions.[29,30] These factors affect the occurrence of CO_2-water-rock reactions, which in turn affect the storage of CO_2. These factors include formation structure, fault presence, rock thickness, porosity, permeability, temperature, pressure, and injection rate, all of which play a significant role in the dynamics of CO_2-water-rock reactions. Eigestad[31] focused on variables such as grid resolution, residual gas saturation, and relative permeability. He conducted a sensitivity analysis to understand how these factors influence CO_2 storage capacities, though without delving into aspects of dissolution and mineralization. In contrast, Wei[32] explored the impact of aspect ratio, hydrodynamic conditions, and injection rates on CO_2 storage, developing a model incorporating hysteresis effects on storage processes. Goater[33] took a different approach by using the Forties saline aquifers in the North Sea as a case study, creating a geological model. The model accounted for variables such as permeability, the angle of the formation bottom, and heterogeneity to assess the CO_2 storage potential of the area. The findings highlighted the significant influence of formation inclination and permeability on CO_2 storage capabilities, due to the long duration and the limitations of experimental conditions. Most of these studies focus on general CO_2 storage. There is limited research on dissolution storage and mineralization storage. However, CO_2 dissolution and mineralization storage are important components of CCS. Therefore, these parts should be studied.

Deep saline aquifers host a diverse array of reservoir minerals, including clay minerals, quartz, potassium feldspar, carbonate minerals, etc. Notably, essential elements like calcium and magnesium predominantly exist in carbonate forms such as calcite and dolomite, with calcite being particularly significant as a reservoir mineral. This study utilizes physical simulation experiments to address the challenges of measuring pH values and other parameters, and applies numerical simulations of CO_2-water-rock reactions to elucidate key influencing parameters. Calcite is a common carbonate mineral in reservoirs. In practical experiments, its reaction effect with CO_2 and water is significant. Therefore, this study takes calcite as the research object. The deep aquifers in the Ordos Basin are widely distributed, and multiple sets of reservoir cap combinations are suitable for CO_2 geological storage. According to previous assessments, the total storage potential of CO_2 in this area is tens of billions of tons, with broad storage prospects. Therefore, the Ordos Basin was chosen as the research object for subsequent numerical simulations. By utilizing physical parameters representative of the Ordos Basin, the study develops a mechanical model, and establishes CO_2 injection wells. This study examines various factors influencing CO_2 storage, primarily focusing on dissolution and mineralization processes. The findings illuminate the impact and underlying mechanisms of reservoir conditions and injection practices on CO_2 storage, particularly in scenarios involving CO_2-water-rock reactions. Due to the slow process and complexity of various chemical

https://doi.org/10.1021/acsomega.4c05620
ACS Omega 2024, 9, 45983−45995

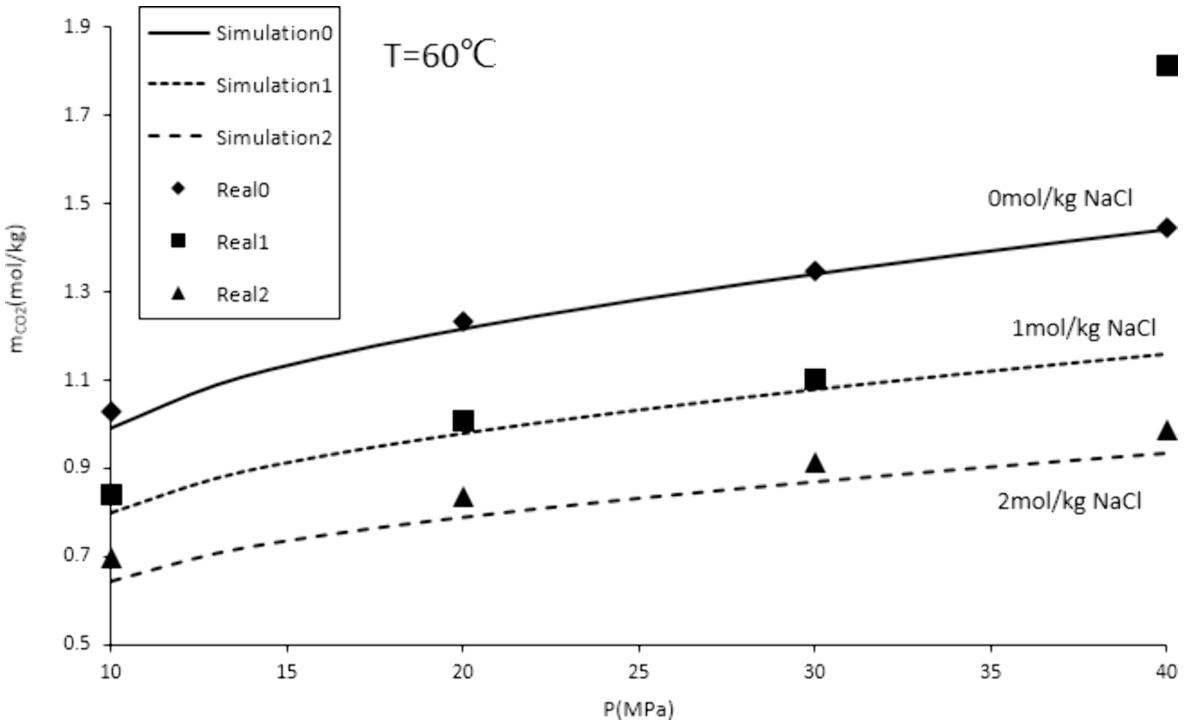

Figure 1. Changes in solubility with pressure under different salinities.

reactions, there is a gap in numerical simulation research in this area. This study aims to bridge this gap, offering valuable insights into the complex dynamics governing CO_2 storage in deep saline aquifers.

2. METHOD

The basic principle of CO_2 storage in saline aquifers is to inject pressurized high-density CO_2 into saline water aquifers through injection wells. CO_2, as an acidic gas, is injected into the deep saline aquifers.[34,35] CO_2 dissolves in water to form carbonic acid under the temperature and pressure of the reservoir, reducing the pH value, and then undergoing geochemical reactions with reservoir minerals.[36] After injecting gaseous CO_2 into the deep saline aquifers, it reacts with water to form carbonic acid. The reaction equations are eq 1 and eq 2.[37]

$$CO_2(g) \rightarrow CO_2(aq) \quad (1)$$

$$H_2O + CO_2(aq) \rightarrow HCO_3^- + H^+ \quad (2)$$

The solubility of CO_2 in water is related to salinity and pressure to a certain extent. This study used the WINPROP module of CMG software, considering the Herry constant and molar volume at infinite dilution, to simulate the changes in solubility with pressure under different salinities at 60 °C. The calculated data from Duan[19] were fitted, and the fitting results are shown in Figure 1.

Figure 1 shows that the simulation results and calculated data have achieved a good fit. As salinity increases, solubility decreases. Solubility increases as pressure increases. Therefore, during the process of CO_2 storage, with the injection of CO_2 and the increase of formation pressure, the solubility of CO_2 will increase.[38,39] After CO_2 dissolves in water, calcite will react with the H^+ produced by CO_2 dissolution to release Ca^{2+}. This reaction will increase the salinity of the solution and reduce the solubility of CO_2. This process is relatively long and may last for thousands of years. The increase in Ca^{2+} concentration in formation water will, generate calcite precipitation, and the reaction equation is eq 3.

$$CaCO_3 + H^+ \Leftrightarrow HCO_3^- + Ca^{2+} \quad (3)$$

The dissolution of CO_2 in formation water causes calcite dissolution to be relatively slow, while the rate of carbonate precipitation reaction between HCO_3^- and Ca^{2+} is relatively fast.

According to the calculation of half wave width, the calcite used in the experiment contains 97.8% $CaCO_3$ and a small amount of $CaMg(CO_3)_2$.[40] Therefore, the purity of the calcite used in this experiment is relatively high, and its main chemical component is $CaCO_3$. The static reaction of CO_2, water, and rock is carried out in a specially designed high-pressure reactor. The calcite flake sample is placed at the bottom of the reactor, and 100 mL of deionized water is poured over the sample.[41] CO_2 is injected into the reactor and reacted at a specific pressure and temperature for 20 days.

When the reaction pressure is 10 MPa, it exceeds the critical pressure of CO_2, and the reaction conditions are approximately in a supercritical state. Using the GEM module of CMG software, establish a one-dimensional model to simulate the dissolution and precipitation reaction of calcite injected with CO_2 under conditions of temperature of 30 °C and pressure of 10 MPa. The fitting situation is shown in Figure 2.

The simulation data and experimental data have achieved a good fit. The relevant parameters of the chemical equilibrium reaction between water, CO_2, and calcite can be obtained, such as reaction rate, specific surface area, and reaction activation energy.

The change in pH during this 20-day reaction process can be determined based on the fitting results.

Figure 3 shows that the pH value first decreases and then increases. With the massive injection of CO_2, it dissolves in water and produces hydrogen ions. These H^+ cause a decrease in

https://doi.org/10.1021/acsomega.4c05620
ACS Omega 2024, 9, 45983−45995

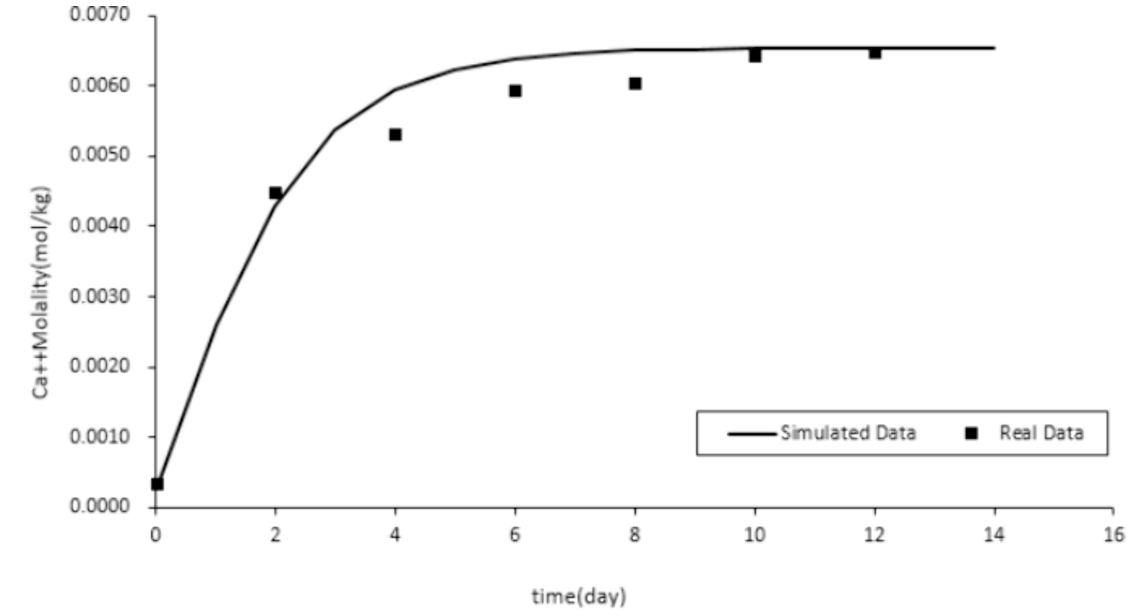

(a)

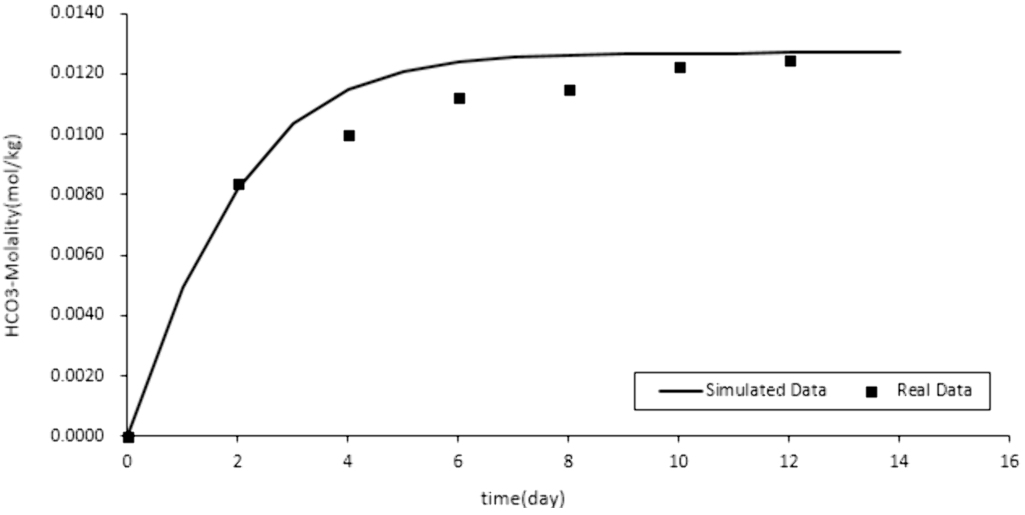

(b)

Figure 2. Simulation data fitting with actual data. (a) Ca^{2+} fitting result. (b) HCO_3^- fitting result.

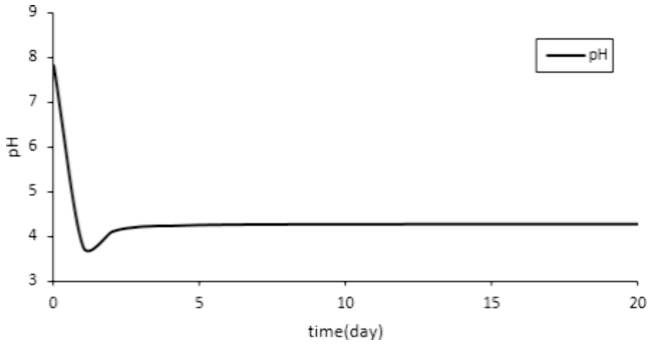

Figure 3. Changes in pH during the 20-day reaction process.

the pH value of the solution.[42] Then, H^+ will react with calcite. The consumption of H^+ will cause the pH to rise until the CO_2-water-rock reaction reaches equilibrium.

The change in porosity during this process can be determined based on the fitting results.

Figure 4 shows that the porosity first increases, then slightly decreases, and then tends to stabilize. Due to the dissolution of calcite, the porosity increases, and then a small portion of calcite precipitates and blocks the pores, resulting in a slight decrease in porosity. However, the precipitation rate is lower than the dissolution rate.[43] Therefore, the porosity decreases slightly until the reaction reaches equilibrium.

3. RESULTS AND DISCUSSION

The CO_2-water-rock reaction significantly impacts the dissolution and mineralization of CO_2. Due to the long time required for mineralization and the complexity of the CO_2-water-rock reaction, previous research has mainly been divided into two types. One is to study the concentration changes of various ions in CO_2-water-rock reaction in actual experiments.

https://doi.org/10.1021/acsomega.4c05620
ACS Omega 2024, 9, 45983−45995

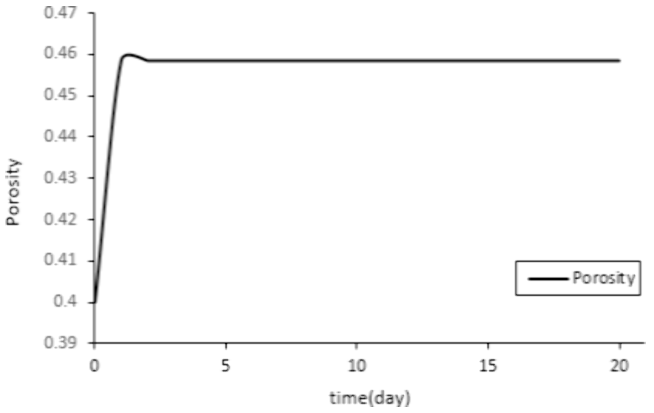

Figure 4. Changes in porosity during the 20-day reaction process.

Table 1. Reservoir Physical Parameters

Permeability (mD)	Porosity	Density of rock (kg/m^3)	Top (m)	Salinity (g/L)
6.58	0.129	2,600	1,700	31.2
Temperature (°C)	Pressure (MPa)	Compressibility (Pa^{-1})	Thickness (m)	pH
60	18.9	4.50×10^{-10}	20	6.5

The second is to simulate the storage process of CO_2 through numerical simulation, and analyze its migration law and storage mechanism. There is relatively little research on the numerical simulation of the CO_2-water-rock reaction.

GEM module of CMG software was used for numerical simulation further to simulate the influencing factors of CO_2 dissolution and mineralization. The simulated block was the deep saline aquifers of the Shiqianfeng Formation in the Ordos Basin.[44,45] A model with $20 \times 20 \times 10$ grids was established, and the CO_2-water-rock reaction only considered calcite. The factors affecting CO_2 dissolution and mineralization were analyzed from two aspects: reservoir conditions and injection process. The reservoir parameters for establishing the model are shown in Table 1.[46−49]

According to previous research, the formation fracture pressure is usually 1.5 times the initial pressure,[50] so it can be concluded that the approximate fracture pressure in the study area is 28.35 MPa. The grid size is 20 m × 20 m × 2 m. It is shown in Figure 5.

This study sets the injection well to stop injecting CO_2 after 20 years. This study simulates a total of 80 years of CO_2 storage. Figure 6 is a cross-sectional view of pH changes over the past 80 years.

Figure 6 shows that the pH value decreases over time. Due to the dissolution of CO_2 in the formation water, releasing H^+ and making the formation water acidic. The pH decreases until the CO_2-water-rock reaction reaches equilibrium, and the pH reaches its minimum value. Figure 7 is a profile map of changes in gas saturation over the past 80 years.

Figure 7 shows that gaseous CO_2 migrates upward under the action of buoyancy, replacing the water in the original reservoir. Figure 8 is a cross-sectional map of the changes in the amount of calcite over the past 80 years.

As time goes by, due to the influence of buoyancy, the range of CO_2 migration above the reservoir is very wide. The range of the reaction of CO_2, water, and calcite occurring is also relatively large. Due to the smaller migration range in the lower part of the reservoir, the CO_2-water-rock reaction time becomes longer, resulting in a relatively large amount of calcite precipitation in the middle and lower parts of the reservoir.

According to relevant information, CO_2 storage can be divided into four types: structural storage (including supercritical CO_2), residual gas storage (including gaseous CO_2),

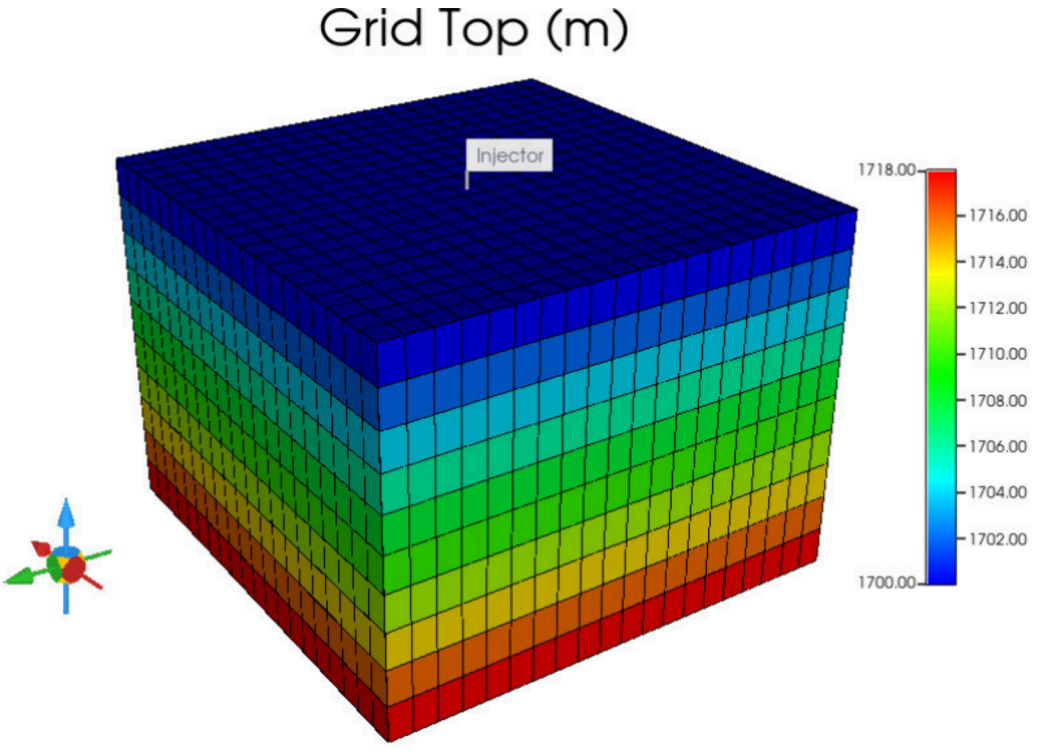

Figure 5. 3D Model.

https://doi.org/10.1021/acsomega.4c05620
ACS Omega 2024, 9, 45983−45995

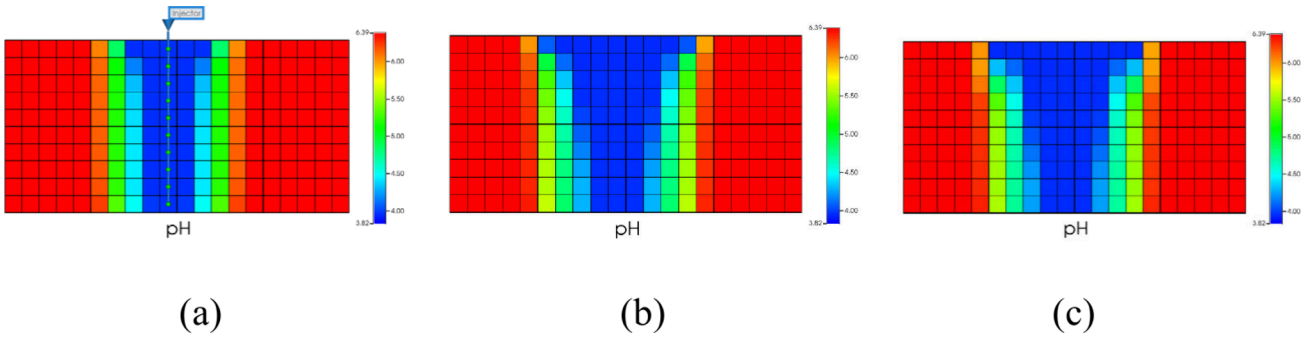

Figure 6. Changes in pH over time. (a) 2 years later. (b) 20 years later. (c) 80 years later.

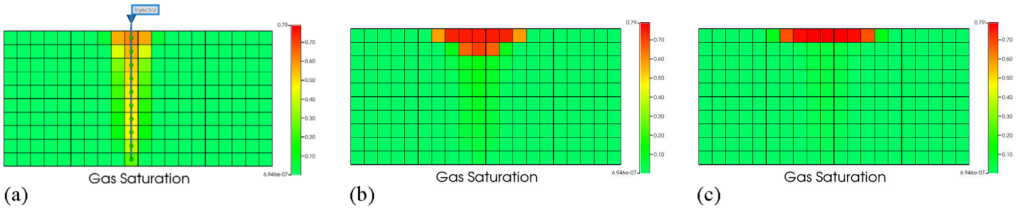

Figure 7. Changes in gas saturation over time. (a) 2 years later. (b) 20 years later. (c) 80 years later.

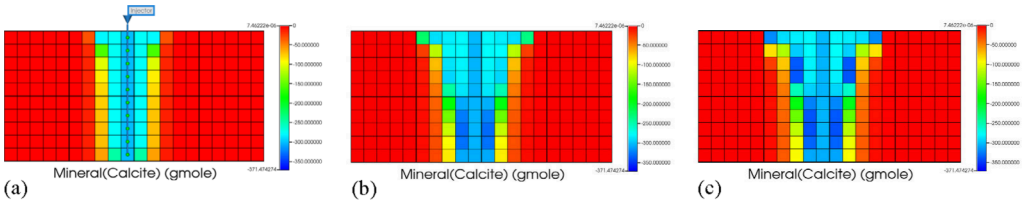

Figure 8. Changes in calcite precipitation over time. (a) 2 years later. (b) 20 years later. (c) 80 years later.

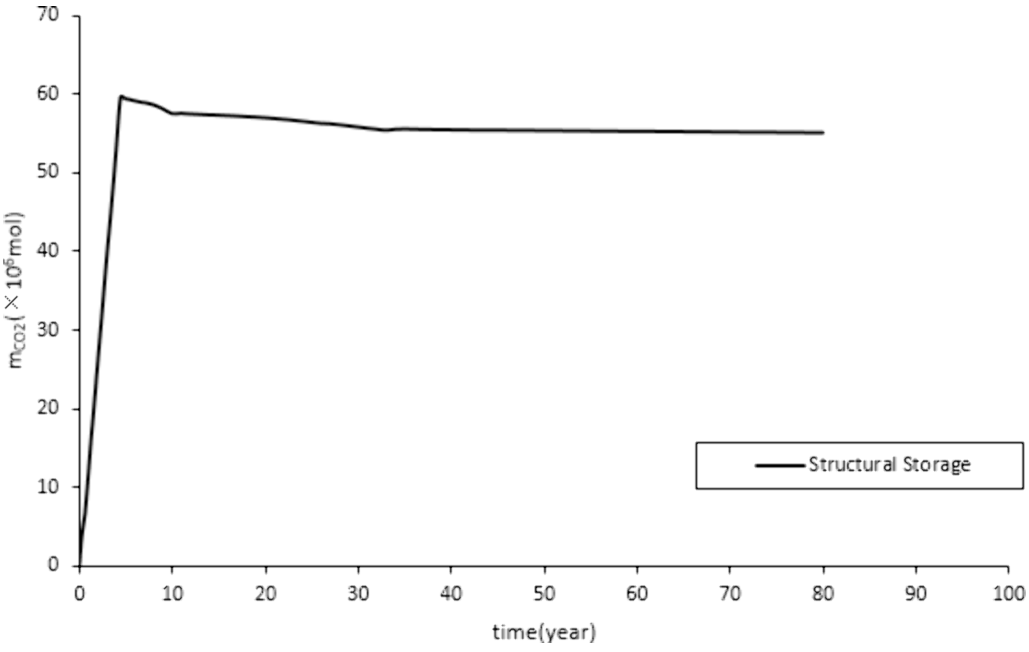

Figure 9. Quantity of structural storage.

dissolved storage (including CO_2 dissolved in water), and mineralized storage (including CO_2 that reacts with minerals). Mineralized storage is divided into mineral storage (dissolution reaction occurs) and aqueous storage (precipitation reaction occurs). CO_2 generates residual gas during injection and formation water reflux processes. The gas stored in this part is called residual gas storage. The factors affecting residual gas storage are the wettability and interfacial tension of the reservoir. This is not in line with the theme of this study. Therefore, considering the accuracy and simplicity of numerical simulation,

https://doi.org/10.1021/acsomega.4c05620
ACS Omega 2024, 9, 45983−45995

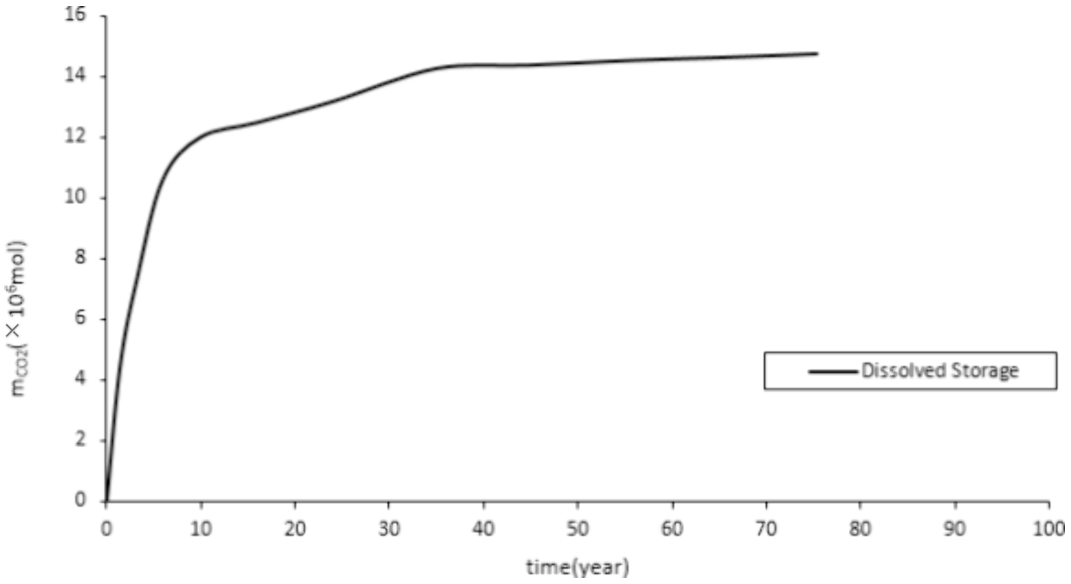

Figure 10. Quantity of dissolved storage.

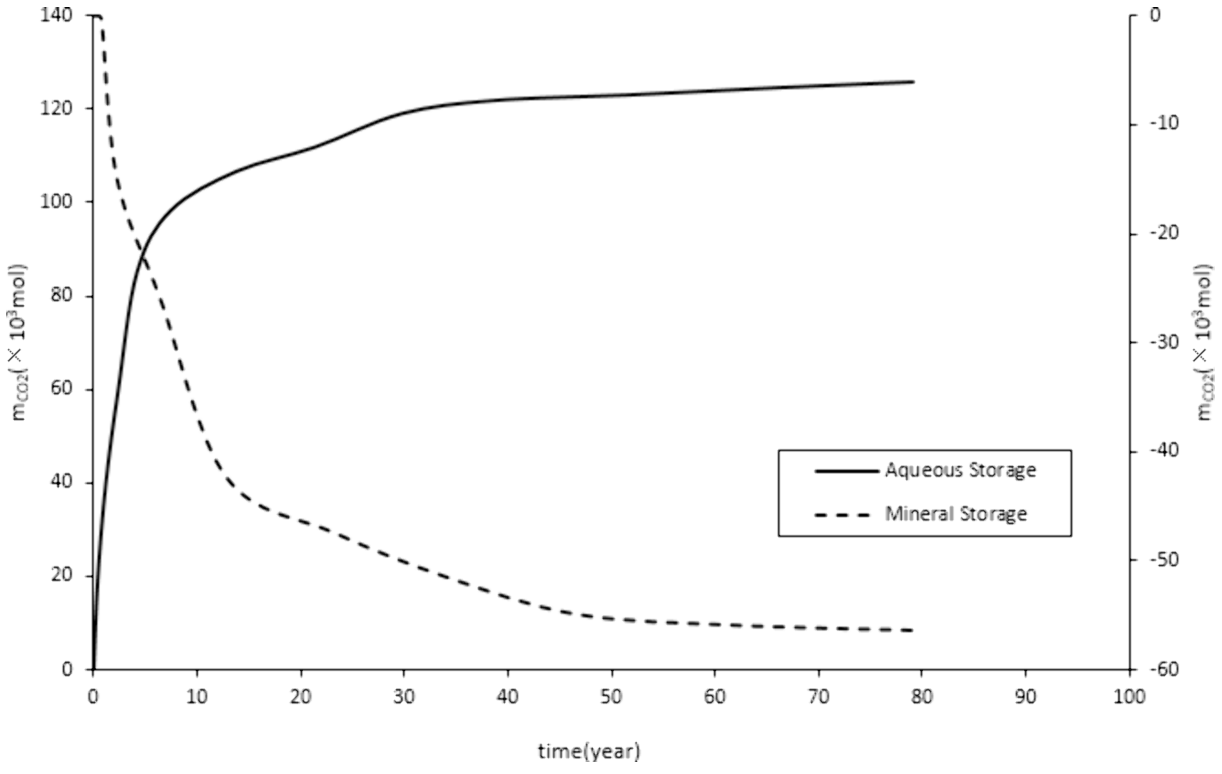

Figure 11. Quantity of mineralized storage.

Table 2. Simulation Schemes for Reservoir Conditions Affecting Storage

Simulation Scheme	Variable	Set value
1	Permeability (mD)	3.29
2		6.58
3		32.9
4		65.8
5	Porosity	0.029
6		0.129
7		0.229
8		0.429

no hysteresis effect will be set in subsequent numerical simulations to obtain residual gas storage. The following are the initial structural storage quantity, dissolved storage quantity, and mineralized storage quantity of this model without changing the parameters.

Figure 10 and Figure 11 show a rapid increase in mineralized and dissolved CO_2 storage, followed by a steady increase. This is due to the rapid increase in formation pressure during the initial stage of CO_2 injection, which promotes the occurrence of the CO_2-water-rock reaction. Therefore, the storage of mineralization and dissolution rapidly increases. Stop CO_2 injection after 20 years. Subsequently, the growth of reserves for mineralization

https://doi.org/10.1021/acsomega.4c05620
ACS Omega 2024, 9, 45983−45995

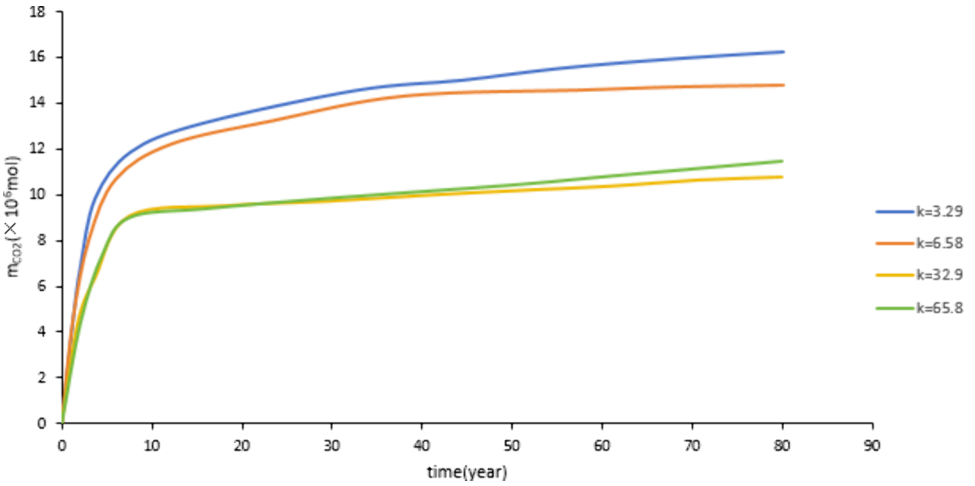

Figure 12. Effect of permeability on dissolved storage.

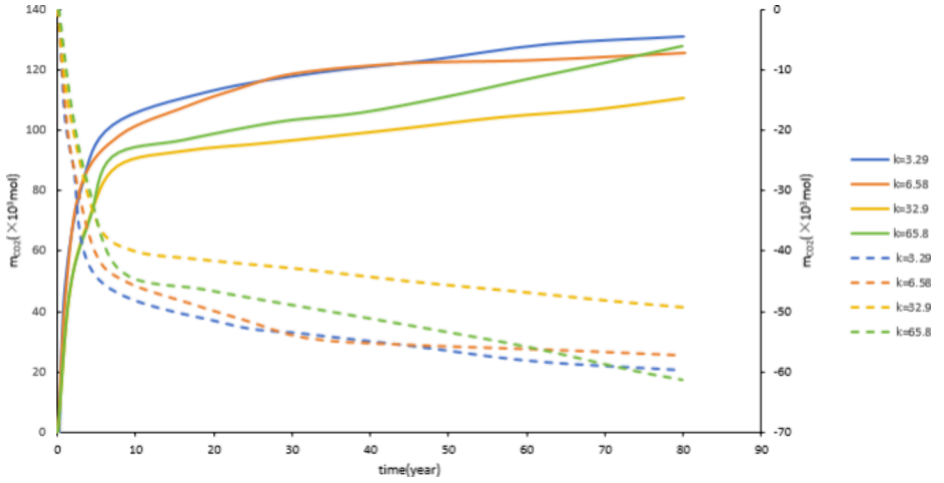

Figure 13. Effect of permeability on mineralized storage.

and dissolution storage mainly relies on a stable CO_2-water-rock reaction, which leads to a stable increase in reserves. CO_2 exists in the form of supercritical gas in the construction of storage. Figure 9 shows that before the production well is shut down, the structural storage increases. Over a long period, a small amount of CO_2 gradually dissolves in the water and undergoes a stable CO_2-water-rock reaction, resulting in a small and stable decrease in the structural storage.

Due to the reverse precipitation generation in eq 3, the mineral storage in this study is shown to be negative.

This study mainly focuses on the effect of the CO_2-water-rock reaction on CO_2 storage, so in subsequent simulations, structural storage will not be considered. Only consider the impact of parameter changes on dissolved and mineralized storage.

3.1. Reservoir Conditions. The volume fraction, permeability, and porosity of minerals and other reservoir conditions may affect the CO_2-water-rock reaction (mineral dissolution or precipitation), thereby affecting a block's CO_2 storage capacity and efficiency.[51−54] In order to clarify permeability (represented in k) and porosity (represented in Φ), the effects on CO_2 dissolution and mineralization were studied as follows. The simulation plan is shown in Table 2.

3.1.1. The Impact of Permeability. As shown in Figure 12 and Figure 13, as the permeability increases from 3.29 mD to 65.8 mD, the CO_2 storage capacity decreases. However, as the permeability increased from 3.29 mD to 6.58 mD, there was a slight decrease in dissolution and mineralization sequestration. When the permeability increases from 32.9 mD to 65.8 mD, both dissolution and mineralization sequestration will increase. The reason for this phenomenon is as follows: the higher the permeability, the stronger the migration ability of CO_2. The wider the range of formation water that CO_2 can come into contact with, the more favorable it is for CO_2 dissolution, increasing the contact surface between CO_2, water, and rock, which is conducive to the occurrence of CO_2 water rock reactions. However, if the permeability continues to increase, it will increase the fluidity of formation water, accelerate the movement speed of CO_2, shorten the reaction time between CO_2 and formation water, and be unfavorable for the occurrence of CO_2 water rock reaction. Therefore, it can be concluded that the permeability should not be too high.

3.1.2. The Influence of Porosity. Figure 14 and Figure 15 show that with the increase of porosity, the dissolved CO_2 and mineralized storage also increase. This is because the larger the porosity, the more formation water is contained in the aquifers, which is more conducive to the dissolution of CO_2. This increases the contact surface between CO_2, water, and rock. It is conducive to CO_2-water-rock reaction. Therefore, an increase in porosity is conducive to dissolved and mineralized storage.

https://doi.org/10.1021/acsomega.4c05620
ACS Omega 2024, 9, 45983−45995

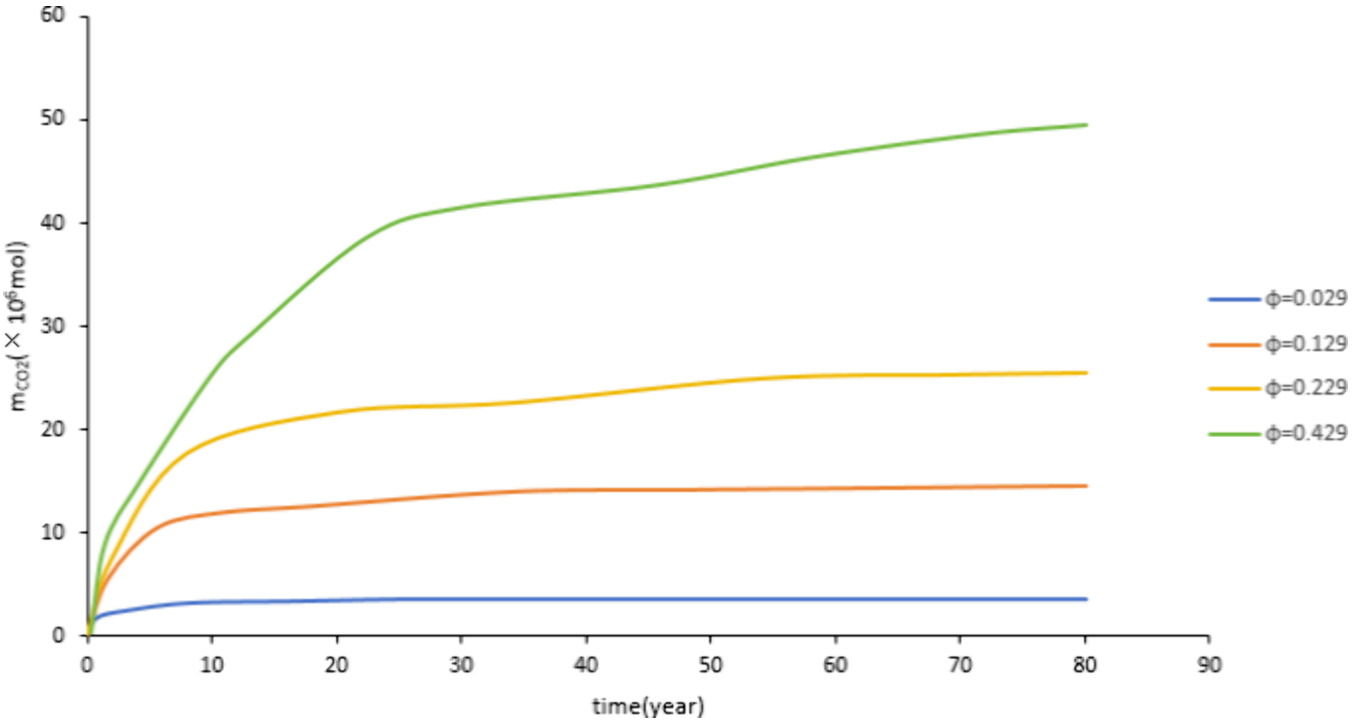

Figure 14. Effect of porosity on dissolved storage.

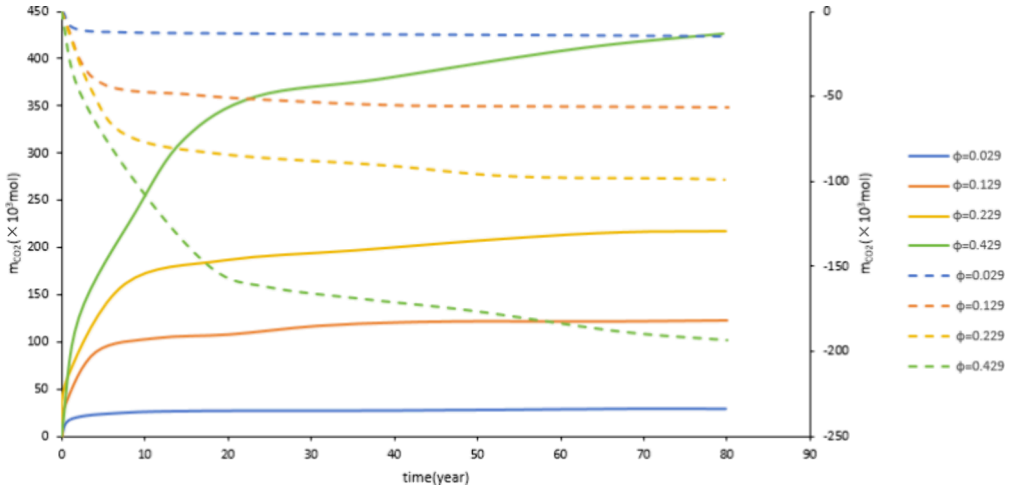

Figure 15. Effect of porosity on mineralized storage.

Table 3. Simulation Schemes for the Impact of Injection Process on Storage[a]

Simulation Scheme	Variable	Set value
1	Injection rate (m^3/d)	500
2		1000
3		2000
4		3000
6	Perforation position	Full
7		Middle (2)
8		Top (2)
9		Bottom (2)

[a]In the middle, top, and bottom, two layers are shot open.

3.2. Implantation Process. Optimizing the injection plan is of great practical significance to achieve large and optimal CO_2 deep saline aquifer storage. The controllable factors for injection include injection temperature, injection rate, perforation position, etc.[55] In order to clarify the impact of injection rate (represented by (v) and perforation position on the dissolution and mineralization of CO_2 in the presence of the CO_2-water-rock reaction, the following research is conducted. The simulation plan is shown in Table 3.

3.2.1. The Impact of Injection Rate. Figure 16 and Figure 17 show that as the injection rate increases, the dissolved CO_2 and mineralized storage increase. As the injection rate increases, the amount of CO_2 in contact with formation water increases, and the migration range of CO_2 increases, which is conducive to CO_2 dissolution and the occurrence of CO_2-water-rock reaction. Therefore, the injection rate increases, and the storage amount increases. During construction, attention should be paid not to exceed the reservoir rupture pressure due to excessive injection volume. Figure 16 and Figure 17 show that as the injection rate increases, the increase in reserves slows down. Therefore,

https://doi.org/10.1021/acsomega.4c05620
ACS Omega 2024, 9, 45983−45995

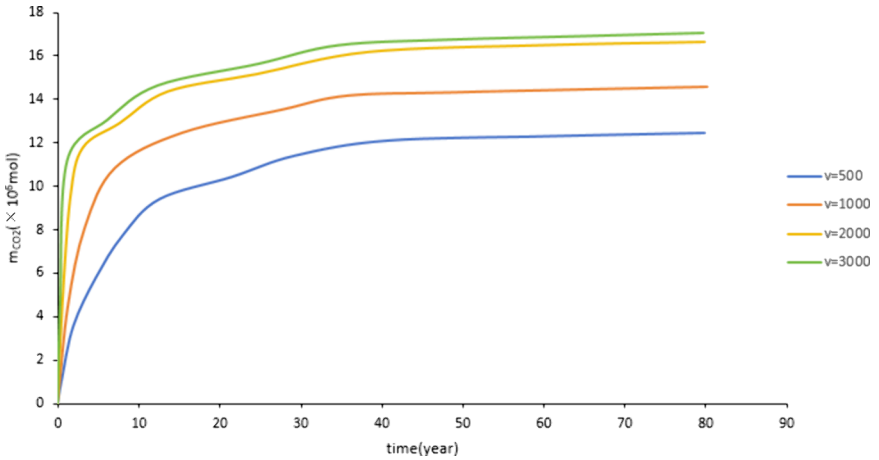

Figure 16. Effect of injection rate on dissolved storage.

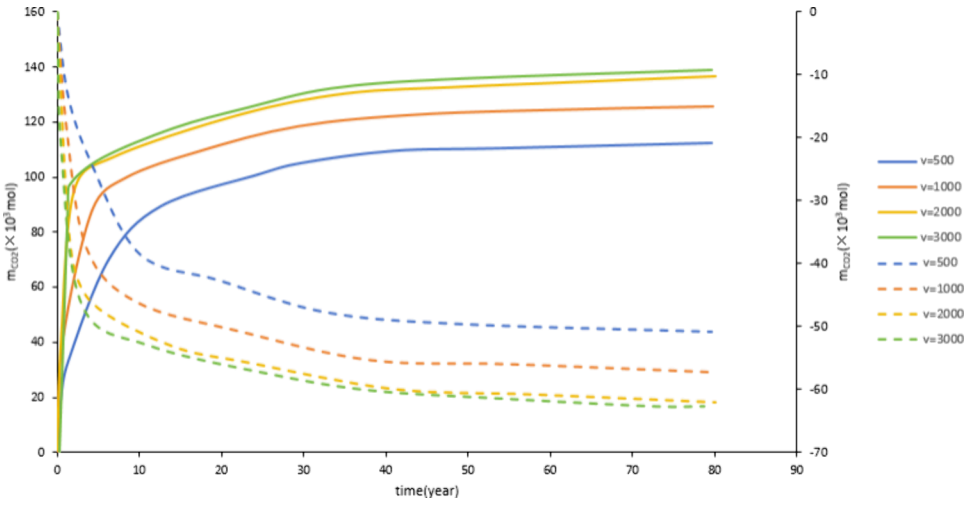

Figure 17. Effect of injection rate on mineralized storage.

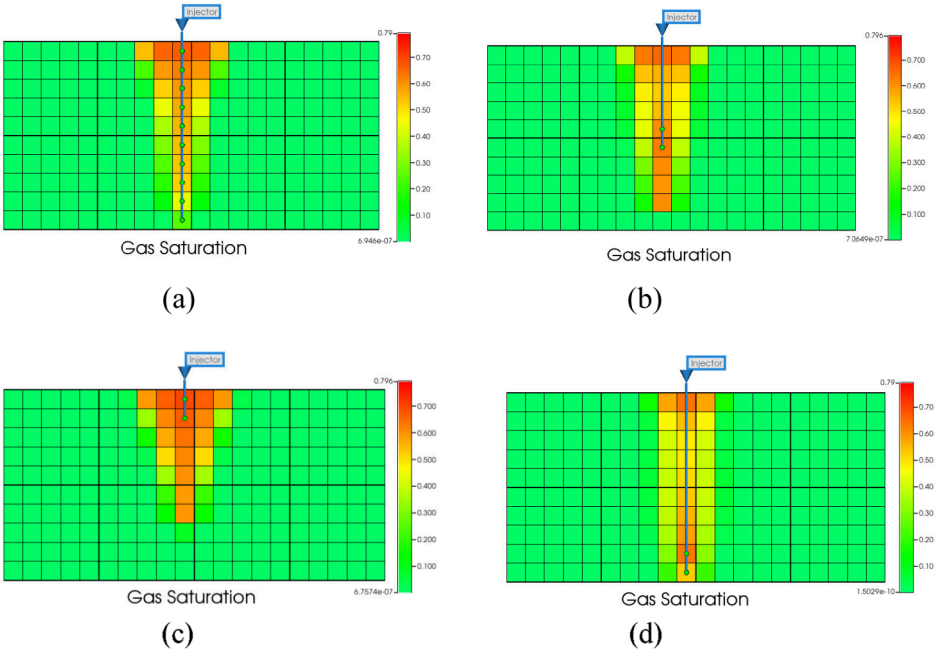

Figure 18. Gas saturation profile. (a) Full layer perforation. (b) Middle layer perforation. (c) Top layer perforation. (d) Bottom layer perforation.

https://doi.org/10.1021/acsomega.4c05620
ACS Omega 2024, 9, 45983−45995

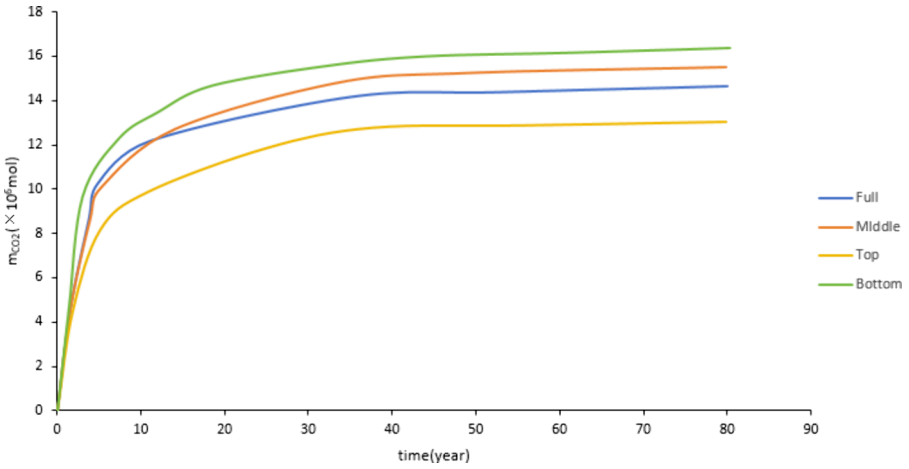

Figure 19. Effect of perforation position on dissolved storage.

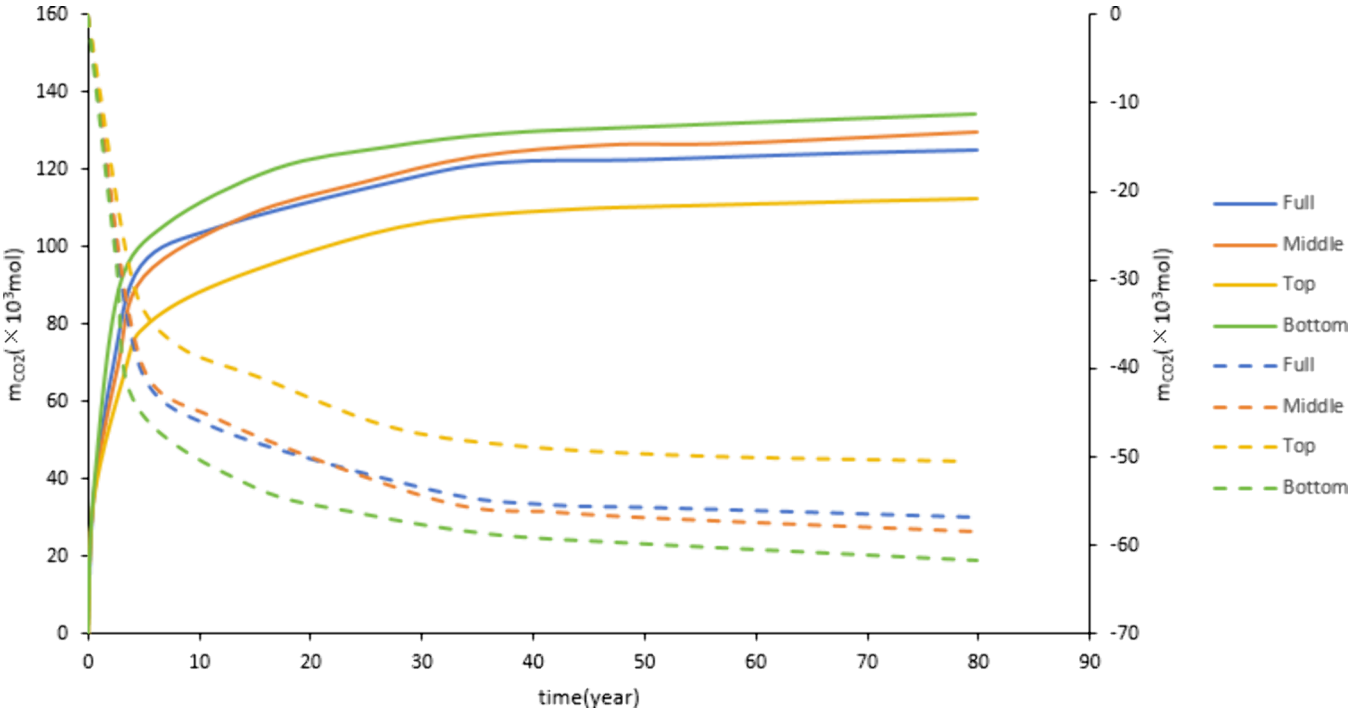

Figure 20. Impact of perforation position on mineralized storage.

considering the cost, an appropriate injection rate should be selected for construction.

3.2.2. The Influence of Perforation Position. Figure 18 shows that the profile of gas saturation after 4 years of CO_2 injection at different perforation positions. It can be seen that the migration range of CO_2 varies greatly at different perforation positions, which can affect the occurrence of CO_2-water-rock reaction.

Figure 19 shows that the CO_2 dissolved storage amount in the bottom perforation is greater than full and middle layer perforation, and the dissolved CO_2 storage amount in the top perforation is the smallest. After CO_2 injection, it will migrate upward due to buoyancy. CO_2 will migrate to the upper part if perforated at the bottom, and the migration range is larger than that of the middle and top perforations. During the migration process, CO_2 can fully contact the formation water, which is conducive to the occurrence of the CO_2-water-rock reaction. At the same injection rate, the injection amount of each layer in the full layer perforation is not as much as in other perforation positions. Therefore, bottom perforation is more conducive to the occurrence of CO_2-water-rock reaction, affecting dissolution and storage. Figure 20 shows that the mineralized storage of the top perforation is smaller than those of the full, middle, and bottom layer perforation. This is due to the buoyancy effect. The CO_2 migration range of the top perforation is smaller than that of other perforation positions, which is not conducive to large-scale CO_2-water-rock reactions. It has a smaller storage capacity.

4. CONCLUSIONS

This study elucidates the significance of CO_2 storage in deep saline aquifers and discusses the common geochemical reactions involved in CO_2 storage processes. This study analyzed the solubility of CO_2 in water. This study obtained the parameters of CO_2, water, and calcite reactions by fitting physical simulation experiments. This study is based on the physical parameters of a certain block in the Ordos Basin, and numerical simulation and

https://doi.org/10.1021/acsomega.4c05620
ACS Omega 2024, 9, 45983−45995

mechanism analysis are conducted on the dissolution and mineralization of CO_2 in the block. The main conclusions are as follows:

1. This study can obtain other parameters that are difficult to measure in practice, such as pH and porosity, by fitting the CO_2-water-rock reaction of calcite.
2. This study obtained the relevant parameters of the CO_2-water-rock reaction by fitting the CO_2-water-rock reaction of calcite.
3. For the studied block, reservoir conditions can affect the CO_2-water-rock reaction, thereby affecting the dissolution and mineralization of CO_2. Permeability should not be too high. The larger the porosity, the more favorable it is for the dissolution and mineralization of CO_2.
4. For the studied block, the injection process will affect the CO_2-water-rock reaction, thereby affecting the dissolution and mineralization of CO_2. In terms of injection rate, the higher the injection rate, the more CO_2 is sequestered. In terms of perforation location, the dissolution and mineralization of CO_2 are larger during bottom perforation.

This study can provide a certain reference for more accurate numerical simulations of CO_2 storage in the future.

AUTHOR INFORMATION

Corresponding Author

Yizhong Zhang − *Petroleum Engineering School and Cooperative Innovation Centre of Unconventional Gas and Oil, Yangtze University, Wuhan 430100, China;* orcid.org/0000-0002-9773-8620; Email: zhangf5y@uregina.ca

Authors

Qingying Zuo − *Petroleum Engineering School and Cooperative Innovation Centre of Unconventional Gas and Oil, Yangtze University, Wuhan 430100, China;* orcid.org/0009-0002-7185-3011

Maolin Zhang − *Petroleum Engineering School and Cooperative Innovation Centre of Unconventional Gas and Oil, Yangtze University, Wuhan 430100, China*

Bin Ju − *Faculty of Petroleum Engineering, Southwest Petroleum University, Chengdu 610500, China*

Wenhui Ning − *Petroleum Engineering School, Yangtze University, Wuhan 430100, China*

Xin Deng − *Petroleum Engineering School, Yangtze University, Wuhan 430100, China*

Long Yang − *Exploration and Development Research Institute of Sinopec Zhongyuan Oilfield Branch, Puyang 457000, China;* orcid.org/0000-0002-9953-2917

Chaofeng Pang − *Petroleum Engineering School and Cooperative Innovation Centre of Unconventional Gas and Oil, Yangtze University, Wuhan 430100, China;* orcid.org/0009-0008-3411-0212

Complete contact information is available at: https://pubs.acs.org/10.1021/acsomega.4c05620

Notes

The authors declare no competing financial interest.

ACKNOWLEDGMENTS

The authors would like to acknowledge the Cooperative Innovation Center of Unconventional Oil and Gas Resources of Yangtze University. We are grateful for the support from the National Natural Science Foundation of China (NSFC grant no.: 52004032)

REFERENCES

(1) Zhang, L.; Wen, R.; Li, F.; Li, C.; Sun, Y.; Yang, H. Assessment of CO_2 mineral storage potential in the terrestrial basalts of China. *Fuel* **2023**, *348*, No. 128602.

(2) Bachu, S. Storage of CO_2 in geological media: criteria and approach for site selection in response to climate change. *Energy conversion and management* **2000**, *41*, 953−970.

(3) Hurlbert, M.; Osazuwa-Peters, M. Carbon capture and storage in Saskatchewan: An analysis of communicative practices in a contested technology. *Renewable and Sustainable Energy Reviews* **2023**, *173*, No. 113104.

(4) Guo, Y.; Li, S.; Sun, H.; Wu, D.; Liu, L.; Zhang, N.; Lu, C.; et al. Enhancing gas production and CO_2 sequestration from marine hydrate reservoirs through optimized CO_2 hydrate cap. *Energy* **2024**, *303*, No. 131821.

(5) Shi, H.; Li, J.; Shen, H.; Li, X.; Wei, N.; Wang, Y.; Pan, H.; et al. Quantitative analysis of the numerical simulation uncertainties from geological models in CO_2 geological storage: A case study of Shenhua CCS project. *International Journal of Greenhouse Gas Control* **2024**, *135*, No. 104142.

(6) Budisa, N.; Schulze-Makuch, D. Supercritical carbon dioxide and its potential as a life-sustaining solvent in a planetary environment. *Life* **2014**, *4*, 331−340.

(7) Goldthorpe, S. Potential for Very Deep Ocean Storage of CO_2 Without Ocean Acidification: A Discussion Paper. *Energy Procedia* **2017**, *114*, 5417−5429.

(8) Zhang, Y.; Zhang, M.; Mei, H.; Zeng, F. Study on salt precipitation induced by formation brine flow and its effect on a high-salinity tight gas reservoir. *J. Pet. Sci. Eng.* **2019**, *183*, No. 106384.

(9) Bemani, A.; Baghban, A.; Mosavi, A.; S, S. Estimating CO_2-Brine diffusivity using hybrid models of ANFIS and evolutionary algorithms. *Engineering Applications of Computational Fluid Mechanics* **2020**, *14*, 818−834.

(10) Chen, X.; Zhang, Q.; Li, Y.; Liu, J.; Liu, Z.; Liu, S.; et al. Investigation on enhanced oil recovery and CO_2 storage efficiency of temperature-resistant CO_2 foam flooding. *Fuel* **2024**, *364*, No. 130870.

(11) Krooss, B. V.; Van Bergen, F.; Gensterblum, Y.; Siemons, N.; Pagnier, H. J. M.; David, P. High-pressure methane and carbon dioxide adsorption on dry and moisture-equilibrated Pennsylvanian coals. *International Journal of Coal Geology* **2002**, *51*, 69−92.

(12) Aghajanloo, M.; Yan, L.; Berg, S.; Voskov, D.; Farajzadeh, R. Impact of CO_2 hydrates on injectivity during CO_2 storage in depleted gas fields: A literature review. *Gas Science and Engineering* **2024**, *123*, No. 205250.

(13) Ali, M.; Jha, N. K.; Pal, N.; Keshavarz, A.; Hoteit, H.; Sarmadivaleh, M. Recent advances in carbon dioxide geological storage, experimental procedures, influencing parameters, and future outlook. *Earth-Science Reviews* **2022**, *225*, No. 103895.

(14) Liu, S.; Zhu, C.; Li, Y.; Hu, S.; Zhang, X.; Ma, C. Mechanism of adsorption capacity enhancement of coal due to interaction with high-pressure $scCO_2$-water system. *Gas Science and Engineering* **2023**, *117*, No. 205080.

(15) Luo, J.; Xie, Y.; Hou, M. Z.; Xiong, Y.; Wu, X.; Lüddeke, C. T.; Huang, L. Advances in subsea carbon dioxide utilization and storage. *Energy Reviews* **2023**, *2*, No. 100016.

(16) Aminnaji, M.; Qureshi, M. F.; Dashti, H.; Hase, A.; Mosalanejad, A.; Jahanbakhsh, A.; Maroto-Valer, M.; et al. CO_2 Gas hydrate for carbon capture and storage applications−Part 1. *Energy* **2024**, *300*, No. 131579.

(17) Mohammadkhani, S.; Fogden, A.; Olsen, D. Fluid-rock interactions during intermittent injection of supercritical CO_2: An investigation for CO_2 storage in the depleted Nini West oil field, Danish North Sea. *International Journal of Greenhouse Gas Control* **2024**, *135*, No. 104141.

(18) Mim, R. T.; Negash, B. M.; Jufar, S. R.; Ali, F. Minireview on CO_2 Storage in Deep Saline Aquifers: Methods, Opportunities, Challenges, and Perspectives. *Energy Fuels* **2023**, *37*, 18467−18484.
(19) Duan, Z.; Sun, R. An improved model calculating CO_2 solubility in pure water and aqueous NaCl solutions from 273 to 533 K and from 0 to 2000 bar. *Chemical geology* **2003**, *193*, 257−271.
(20) Kaszuba, J. P.; Janecky, D. R.; Snow, M. G. Carbon dioxide reaction processes in a model brine aquifer at 200°C and 200 bar: implications for geologic storage of carbon. *Applied geochemistry* **2003**, *18*, 1065−1080.
(21) Lahann, R.; Mastalerz, M.; Rupp, J. A.; Drobniak, A. Influence of CO_2 on New Albany Shale composition and pore structure. *International Journal of Coal Geology* **2013**, *108*, 2−9.
(22) Luhmann, A. J.; Kong, X. Z.; Tutolo, B. M.; Garapati, N.; Bagley, B. C.; Saar, M. O.; Seyfried, W. E., Jr Experimental dissolution of dolomite by CO_2-charged brine at 100 C and 150 bar: Evolution of porosity, permeability, and reactive surface area. *Chem. Geol.* **2014**, *380*, 145−160.
(23) Duan, Z.; Sun, R.; Zhu, C.; Chou, I. M. An improved model for the calculation of CO_2 solubility in aqueous solutions containing Na^+, K^+, Ca^{2+}, Mg^{2+}, Cl^-, and SO_4^{2-}. *Marine chemistry* **2006**, *98*, 131−139.
(24) Gunter, W. D.; Perkins, E. H.; Hutcheon, I. Aquifer disposal of acid gases: modelling of water−rock reactions for trapping of acid wastes. *Appl. Geochem.* **2000**, *15*, 1085−1095.
(25) Xu, T.; Apps, J. A.; Pruess, K. Mineral storage of carbon dioxide in a sandstone−shale system. *Chemical geology* **2005**, *217*, 295−318.
(26) Cantucci, B.; Montegrossi, G.; Vaselli, O.; Tassi, F.; Quattrocchi, F.; Perkins, E. H. Geochemical modeling of CO_2 storage in deep reservoirs: The Weyburn Project (Canada) case study. *Chem. Geol.* **2009**, *265*, 181−197.
(27) Ranganathan, P.; van Hemert, P.; Rudolph, E. S. J.; Zitha, P. Z. Numerical modeling of CO_2 mineralisation during storage in deep saline aquifers. *Energy Procedia* **2011**, *4*, 4538−4545.
(28) Davoodi, S.; Al-Shargabi, M.; Wood, D. A.; Rukavishnikov, V. S.; Minaev, K. M. Review of technological progress in carbon dioxide capture, storage, and utilization. *Gas Science and Engineering* **2023**, *117*, No. 205070.
(29) Li, Z.; Su, Y.; Shen, F.; Huang, L.; Ren, S.; Hao, Y.; Fan, Y.; et al. Investigation of CO_2 storage and EOR of alternating N_2 and CO_2 injection using experiments and numerical simulation. *Fuel* **2023**, *340*, No. 127517.
(30) Xie, J.; Yang, X.; Qiao, W.; Peng, S.; Yue, Y.; Chen, Q.; Liu, Y.; et al. Investigations on CO_2 migration and flow characteristics in sandstone during geological storage based on laboratory injection experiment and CFD simulation. *Gas Science and Engineering* **2023**, *117*, 205058−205058.
(31) Eigestad, G. T.; Dahle, H. K.; Hellevang, B.; Riis, F.; Johansen, W. T.; et al. Geological modeling and simulation of CO_2 injection in the Johansen formation. *Computational Geosciences* **2009**, *13*, 435−450.
(32) Wei, L.; Saaf, F. Estimate CO_2 storage capacity of the Johansen formation: numerical investigations beyond the benchmarking exercise. *Computational Geosciences* **2009**, *13*, 451−467.
(33) Goater, A. L.; Bijeljic, B.; Blunt, M. J. Dipping open aquifers—The effect of top-surface topography and heterogeneity on CO_2 storage efficiency. *International Journal of Greenhouse Gas Control* **2013**, *17*, 318−331.
(34) Liu, Z.; Xu, J.; Li, H.; Li, S.; Fan, X. Numerical Investigation of CO_2 Storage Capacity via Hydrate in Deep-Sea Sediments. *Energy Fuels* **2023**, *37*, 18996−19010.
(35) Dong, W.; Li, Z.; Shen, L.; Liu, W.; Guo, Y.; Xu, H.; Yong, R. Study on the process of mass transfer and deterioration of limestone under dynamic dissolution of CO_2 solution. *Sci. Rep.* **2024**, *14*, 5278.
(36) Anwar, M. N.; Fayyaz, A.; Sohail, N. F.; Khokhar, M. F.; Baqar, M.; Khan, W. D.; Nizami, A. S.; et al. CO_2 capture and storage: A way forward for sustainable environment. *Journal of environmental management* **2018**, *226*, 131−144.
(37) Zhang, L.; Wen, R.; Geng, S.; Shi, X.; HAO, Y.; Ren, S. Mineral trapping of CO_2 in basalt rock: Progress and key issues. *Journal of Chemical Engineering of Chinese Universities* **2022**, *36*, 473−480. [In Chinese]
(38) Khudaida, K. J.; Das, D. B. A numerical analysis of the effects of supercritical CO_2 injection on CO_2 storage capacities of geological formations. *Clean Technologies* **2020**, *2*, 21.
(39) Mondal, M. K.; Balsora, H. K.; Varshney, P. Progress and trends in CO_2 capture/separation technologies: A review. *Energy* **2012**, *46*, 431−441.
(40) Xiao, N.; Li, S.; Lin, M. The influence of CO_2 -water-calcite reactions on surface texture and permeability of the calcite. *Science Technology and Engineering* **2017**, *17*, 38−44. [In Chinese]
(41) Yu, M.; Liu, L.; Yang, S.; Yu, Z.; Li, S.; Yang, Y.; Shi, X. Experimental identification of CO_2−oil−brine−rock interactions: Implications for CO_2 storage after termination of a CO_2-EOR project. *Applied geochemistry* **2016**, *75*, 137−151.
(42) Chen, S.; Wang, H.; Wang, H.; Guo, W.; Xiushan, L. Strip Coal Pillar Design Based on Estimated Surface Subsidence in Eastern China. *Rock Mechanics and Rock Engineering* **2016**, *49*, 3829−3838.
(43) Qin, J.; Zhong, Q.; Tang, Y.; Rui, Z.; Qiu, S.; Chen, H. CO_2 storage potential assessment of offshore saline aquifers in China. *Fuel* **2023**, *341*, No. 127681.
(44) Ren, D.; Wang, X.; Kou, Z.; Wang, S.; Wang, H.; Wang, X.; Zhang, R.; et al. Feasibility evaluation of CO_2 EOR and storage in tight oil reservoirs: a demonstration project in the Ordos Basin. *Fuel* **2023**, *331*, No. 125652.
(45) Guo, J.; Wen, D.; Zhang, S.; Xu, T.; Li, X.; Diao, Y.; Jia, X. Potential and Suitability Evaluation of CO_2 Geological Storage in Major Sedimentary Basins of China, and the Demonstration Project in Ordos Basin. *Acta Geologica Sinica* **2015**, *89*, 1319−1332.
(46) Li, C.; Zhang, K.; Wang, Y.; Guo, C.; Maggi, F. Experimental and numerical analysis of reservoir performance for geological CO_2 storage in the Ordos Basin in China. *International Journal of Greenhouse Gas Control* **2016**, *45*, 216−232.
(47) Li, Y.; Li, P.; Qu, H. J.; Wang, G. W.; Sun, X. H.; Ma, C.; Yao, T. X. Potential evaluation of saline aquifers for the geological storage of carbon dioxide: A case study of saline aquifers in the Qian-5 member in northeastern Ordos Basin. *China Geology* **2024**, *7*, 12−25.
(48) Oldenburg, C. M.; Pruess, K.; Benson, S. M. Process modeling of CO_2 injection into natural gas reservoirs for carbon storage and enhanced gas recovery. *Energy Fuels* **2001**, *15*, 293−298.
(49) Tao, J.; Meng, S.; Li, D.; Rui, Z.; Liu, H.; Xu, J. Analysis of CO_2 effects on porosity and permeability of shale reservoirs under different water content conditions. *Geoenergy Science and Engineering* **2023**, *226*, No. 211774.
(50) Amarasinghe, W.; Fjelde, I.; Guo, Y. CO_2 dissolution and convection in oil at realistic reservoir conditions: A visualization study. *Journal of Natural Gas Science and Engineering* **2021**, *95*, No. 104113.
(51) Rutqvist, J.; Birkholzer, J.; Cappa, F.; Tsang, C.-F. Estimating maximum sustainable injection pressure during geological storage of CO_2 using coupled fluid flow and geomechanical fault-slip analysis. *Energy Conversion and Management* **2007**, *48*, 1798−1807.
(52) Liu, H.; Hou, Z.; Were, P.; Gou, Y.; Sun, X. Simulation of CO_2 plume movement in multilayered saline formations through multilayer injection technology in the Ordos Basin, China. *Environmental earth sciences* **2014**, *71*, 4447−4462.
(53) Zare Reisabadi, M.; Sayyafzadeh, M.; Haghighi, M. Stress and permeability modelling in depleted coal seams during CO_2 storage. *Fuel* **2022**, *325*, No. 124958.
(54) Zhang, Y.; Ju, B.; Zhang, M.; Wang, C.; Zeng, F.; Hu, R.; Yang, L. The Effect of Salt Precipitation on the Petrophysical Properties and the Adsorption Capacity of Shale Matrix based on the Porous Structure Reconstruction. *Fuel* **2022**, *310*, No. 122287.
(55) Liu, H.; Hou, Z.; Were, P.; Gou, Y.; Sun, X. Numerical investigation of the formation displacement and caprock integrity in the Ordos Basin (China) during CO_2 injection operation. *J. Pet. Sci. Eng.* **2016**, *147*, 168−180.

https://doi.org/10.1021/acsomega.4c05620
ACS Omega 2024, 9, 45983−45995